3rd EUROPEAN CONFERENCE ON
EARTHQUAKE ENGINEERING & SEISMOLOGY
BUCHAREST, ROMANIA, 2022

Towards improved response quantification of existing infilled RC frames

Gerard J. O'Reilly – Assistant Professor, Scuola Universitaria Superiore IUSS Pavia, Italy, E-mail: gerard.oreilly@iusspavia.it

Al-Mouayed B. Nafeh – PhD Candidate, Scuola Universitaria Superiore IUSS Pavia, Italy, E-mail: mouayed.nafeh@iusspavia.it

Abstract: When assessing the seismic performance of existing structures, the probabilistic distribution of the response is quantified with respect to some form of seismic intensity measure (IM). IMs are usually defined in terms of ground shaking characteristics and a structure's dynamic properties, with spectral acceleration at the first mode of vibration, $Sa(T_1)$, or peak ground acceleration (PGA) being popular choices for buildings. In existing reinforced concrete (RC) buildings with masonry infill panels, a common typology in the Mediterranean area, the increased stiffness and relative brittleness of these panels notably modify structural behaviour, especially in older buildings where no seismic design provisions were utilised. Abrupt changes in stiffness and strength due to local infill panel failure and subsequent non-ductile mechanisms can render IMs like $Sa(T_1)$ poor and possibly biased response predictors. This paper explores an improved IM in $Sa_{avg}(T^*)$ for RC buildings with masonry infill panels from the perspective of efficient and unbiased response prediction. A detailed case-study building is examined to show that simple IMs like PGA and $Sa(T_1)$ are not bad estimators of response but can be prone to losing much of their predictive power - to an extent that other IMs begin to govern - resulting in increased uncertainty and potential bias.

Keywords: PBEE; fragility; intensity measure; bias; assessment.

1. Introduction

Engineers utilise an intensity measure (IM), which is the interface parameter linking seismological and engineering aspects (Bradley 2012), to examine the response of structures and evaluate seismic performance. Obtaining an accurate evaluation of performance is particularly important in the estimation of risk and possible consequences in structures, such as industrial facilities and the impacts in terms of worker safety and their safe navigation and egress explored in the ROSSINI project (O'Reilly et al. 2022). Past studies note that an IM should possess the attributes of practicality, sufficiency and efficiency. It is implied that the adopted IM is a comprehensive descriptor of structural response (i.e., efficient) and that other parameters do not have a notable influence, or bias, on the response estimates. This differs from sufficiency and relates to other ground-shaking characteristics and their potential to bias the results.

In the case of non-ductile reinforced concrete (RC) frames with masonry infill panels, elongation of the initial undamaged first mode period of vibration, T_1, is typically expected due to the local collapse of infill walls (Nafeh, O'Reilly, and Monteiro 2020). This results in a notable strength degradation and subsequent period elongation before the eventual global collapse, which is of notable importance when using $Sa(T_1)$ as the IM. Furthermore, the peak ground acceleration (PGA) is also known to be somewhat an inefficient predictor (Rossetto and Elnashai 2003), given its lack of a direct relationship to modal properties.

This study examines IMs for infilled RC frame structures, with a particular focus on improved efficiency and reduced bias in results. A case-study building located in Southern Italy is examined in detail with $Sa(T_1)$, PGA, and another IM known as average spectral acceleration, $Sa_{avg}(T^*)$, being utilised. The response of the structure is described in detail and the results are scrutinised in terms of their efficiency and potential to be biased by other ground motion parameters.

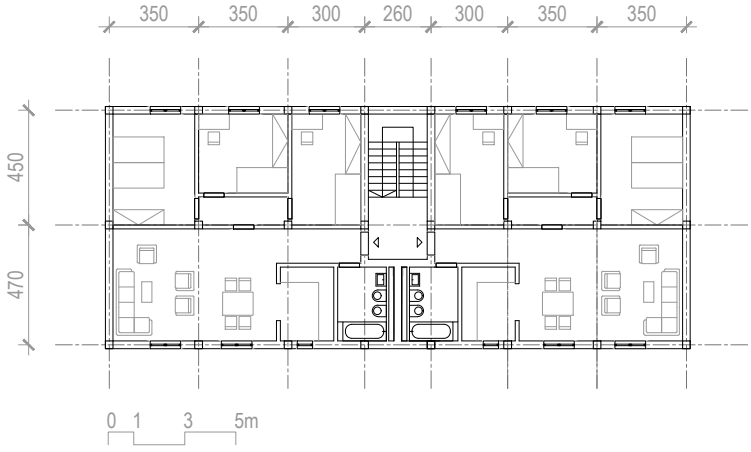

Figure 1. Architectural plan layout of the 4-storey case-study building

2. Case-study building

2.1. Description

The case study building, whose plan layout is illustrated in Figure 1, was a moment-resisting infilled frame RC structure designed for gravity loads only, representative of European structures before the introduction of modern seismic provisions around the 1970s. Smooth rebars (Aq42) and low concrete grade with allowable stresses corresponding to 33% of the material resistance - $\sigma_{s,allowable}$=140MPa for steel and $\sigma_{c,allowable}$=5MPa for concrete - were considered as per the provisions used at the time in Italy (Regio Decreto 1939). Frames were oriented along the global Y-direction only, with only perimeter frames in the X-direction. Beam sections were 50x30cm with reinforcement ratios of ρ_{beam}=0.21-0.41% and column sections were 40x40cm on the first storey and 35x35cm from the second storey to roof level with ρ_{column}=0.75-0.89%. Beams and columns were, compared with modern code requirements, inadequately designed for shear via transverse reinforcement, with 6mm bars at 150mm and 200mm spacing were considered for beams and columns, respectively.

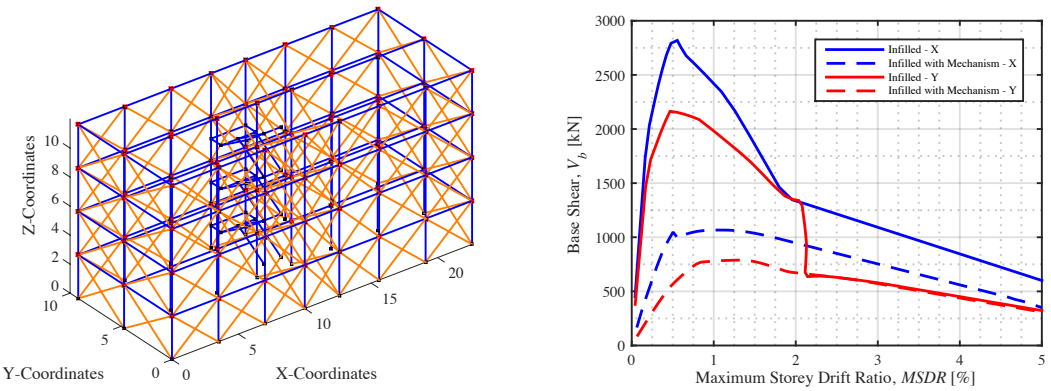

Figure 2. (left) OpenSees model of the 4-storey case-study building and (right) static pushover analysis in the X and Y directions considering the infilled frame with and without a soft-storey mechanism induced

A 3D lumped plasticity model was developed in OpenSees and is shown in Figure 2(left). Beam-column elements were modelled with bi-directional flexural sections with an internal elastic element behaviour with cracked section properties via models by (O'Reilly and Sullivan 2019); the shear capacity of RC elements was modelled using shear springs. Beam-column joints were modelled to account for insufficient joint reinforcement and smooth bars with end-hooks.

2.2. Modal response and pushover analysis

First, a modal analysis revealed a first mode dominated behaviour in both directions (Table 1). To characterise the non-linear behaviour of the case-study building, a first mode-based static pushover analysis was conducted in both principal directions. Figure 2(right) shows the response, where the increased lateral strength and stiffness due to the presence of masonry infills is clear. The structural behaviour is characterised by a sudden drop in capacity in the post-peak branch of the response following the local collapse of infill panels. Also plotted in Figure 2(right) is the same structure modelled with no infill panels at the storey where the infill collapse mechanism would be expected to form. This is anticipated to be representative of the hysteretic behaviour of the building during subsequent cycles following the local collapse of infills at one or more storeys. Furthermore, the sudden drop in lateral capacity in the Y-direction at a drift of just over 2% corresponds to a brittle shear failure caused by the short column effect due to the addition of stairs and further highlights the fragile nature of the collapse mechanisms formed. The short-column effect was captured through the discretisation of staircase columns at the landing and flight elevations.

Table 1. Modal properties

Period, T	Direction	Modal Mass, M
0.22s	X-1	83.6%
0.24s	Y-1	83.2%
0.09s	X-2	10.4%
0.19s	Y-2	13.4%

3. Intensity measures and record selection

3.1. Intensity measures

For this study, three IMs were examined:

- *PGA* – defined as the peak ground acceleration of a given ground motion record;
- $Sa(T^*)$ – the 5%-damped pseudo-spectral acceleration at T^*, which was computed as the arithmetic mean of the X and Y direction first mode periods;
- $Sa_{avg}(T^*)$ – the average spectral acceleration ranging from T_{lower} and T_{upper} of a given record.

PGA is a self-explanatory quantity and $Sa(T^*)$ is intended to closely correspond to the spectral acceleration at the first mode period of vibration in both directions of the building. This was computed from Table 1 as $T^* = (0.22+0.24)/2 = 0.23$s. For $Sa_{avg}(T^*)$, the geometric mean of the $Sa(T)$ values in the period range $[T_{lower}, T_{upper}]$ with a spacing of 0.1s was utilised. T_{lower} and T_{upper} were defined following the rationale outlined for non-ductile infilled RC frames in O'Reilly (2021) as 0.24s and 0.73s, respectively.

3.2. Site hazard and record selection

The case-study building is located at Campobasso in the region of Molise in southern Italy, characterised by moderately high seismicity. Probabilistic seismic hazard analysis (PSHA)

and disaggregation were conducted in OpenQuake considering a $V_{s,30}$=480m/s for each of the IMs examined herein (*PGA*, *Sa*(*T**) and $Sa_{avg}(T^*)$). For each IM, ground motion record selection was performed. Thirty ground motion record pairs were selected and scaled for discrete intensity levels to carry out MSA and characterise the structural response. The conditional spectrum (CS) approach (Jayaram, Lin, and Baker 2011) was followed for *Sa*(*T**) and *PGA*, whereas its extension to $Sa_{avg}(T^*)$-based selection by Kohrangi et al. (2017) was used. The geometric mean of the two components was used in the selection. Seven intensity measure levels (IMLs) were investigated ensuring that the structural response covering initial damage of the masonry infill panels up to global structural collapse could be characterised.

4. Results

4.1. Multiple stripe analysis

The engineering demand parameter (EDP) used was the maximum absolute value along the building height of the peak transient storey drifts, with the greater of the X or Y direction being utilised and denoted θ_{max}, and described in Eq. *(1)*; $|\theta_{i,j}(t)|$ denotes the absolute value of storey drift at time *t* in the principal direction *i* at storey *j*, for a building of *N* storeys and a record of duration t_{max}. Cases were separated into collapsing and non-collapsing cases, where collapse indicates a complete loss of lateral capacity, with $\theta_{collapse}$=5% being used.

$$\theta_{max} = \max_{\substack{i=X,Y \\ j=1\ldots N \\ t=0..t_{max}}} \left|\theta_{i,j}(t)\right| \tag{1}$$

Figure 3(left) illustrates the data obtained for the three IMs examined. The response points for each MSA stripe are shown to be tightly bound at low intensities, followed by an increase in dispersion amongst the points with increasing intensity measure levels (IML). This has been noted in past work (O'Reilly and Monteiro 2019) to result from the characteristic response of infilled RC frames. Initially, the structure behaves in a somewhat typical, first mode-based manner, with demands distributed along the height. Upon damage and collapse of the masonry infill panels in one or more storeys due to its non-ductile behaviour, a significantly modified dynamic response results thereafter, observed by the concentration of damage in the weaker storey(s), which is reflected via its period elongation.

4.2. Fragility functions

For each MSA stripe, if the fraction of exceedances for a given EDP threshold at each of the IMLs are counted (i.e., a vertical cut in the data shown in Figure 3(left)), a fragility function may be fitted using the maximum likelihood method, with a lognormal distribution assumed. Doing this for the collapse threshold yields the collapse fragility function shown in Figure 3(right) for each IM. Of note is the dispersion between the different IMs, with *Sa*(*T**) illustrating the highest dispersion. Also shown in the comparison for the *Sa*(*T**) collapse fragility derived from MSA and the one obtained for the extended SPO2IDA tool (Nafeh, O'Reilly, and Monteiro 2020) which simply uses the pushover curves shown in Figure 2(right) as input, and demonstrates a good match.

Performing the same operation for a range of EDP or θ_{max} values gives a series of fragility functions describing the exceedance of any θ_{max} value in the building with respect to IML. Of particular interest when evaluating the three IMs in question is the dispersion in these fragility functions. Namely, the dispersion in intensity for a given value of EDP, $\beta_{IML|EDP}$, which is an indicator of the efficiency of the IM, is illustrated in Figure 4(left). It can be seen how initially *Sa*(*T**) appears to have the lowest dispersion, owing to its close relationship to

the initial elastic behaviour of the building, whereas *PGA* is seen to be rather high, with $Sa_{avg}(T^*)$ appearing to be somewhere between the two. What is interesting to note is for increasing θ_{max} in the case-study building, *PGA* appears to remain relatively inefficient and $Sa_{avg}(T^*)$ remains relatively consistent. $Sa(T^*)$, however, appear to lose its efficiency with increasing drift demand.

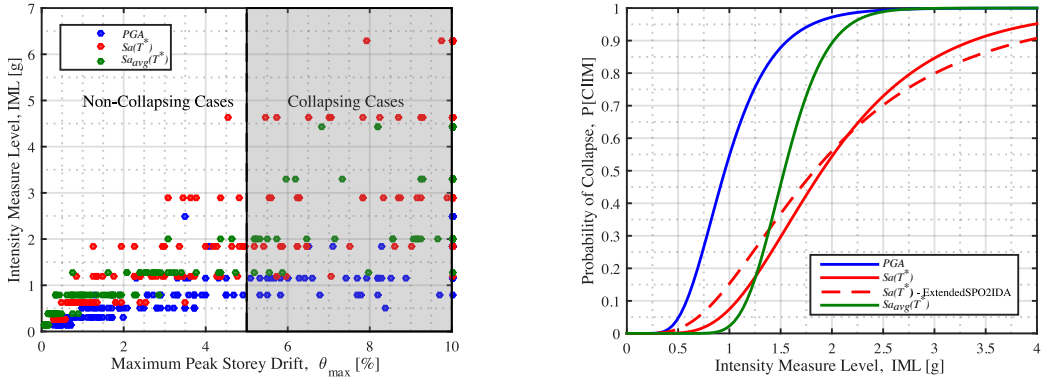

Figure 3. (left) MSA results and (right) illustration of the collapse fragility functions derived from MSA for each of the IMs

Hence, based on the results presented in Figure 4(left), it appears that the traditionally adopted IMs of *PGA* and $Sa(T^*)$ typically used in the past for building structures may not be the most efficient means of quantifying the structural response, with $Sa_{avg}(T^*)$ reporting a lower and more consistent efficiency for all levels of drift demand. It is noted that the remarks made regarding the IMs efficiency have only been examined for displacement-based EDPs and other force-based EDPs, like member force or peak floor acceleration, have not been considered.

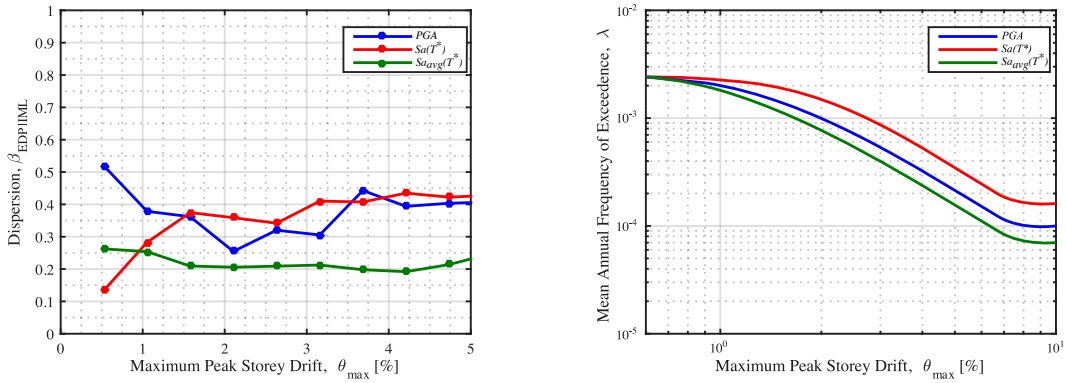

Figure 4. (left) Illustration of the dispersion in the intensity measure level for a given demand, $\beta_{IML|EDP}$ for each IM investigated and (right) demand-hazard curve for each IM, showing the MAFE with increasing drift demand

4.3. Risk

When constructing the fragility functions, the median intensity, $\eta_{IML|EDP}$, and $\beta_{IML|EDP}$ of the IMLs required to exceed a given EDP level were characterised for each IM at increasing levels of structural demand. This can be integrated directly with each IM's hazard curve to compute the mean annual frequency of exceedance (MAFE) of an EDP, λ, as follows:

$$\lambda = \int_0^{+\infty} \Phi\left[\frac{\ln s - \eta_{IML|EDP}}{\beta_{IML|EDP}}\right] |dH(s)| \tag{2}$$

where $\Phi[\bullet]$ denotes the standard normal cumulative distribution function.

To evaluate the different IM estimates of λ, it is typical to look for the consistency between them. This stems from the findings of Bradley (2012), subsequently supported by Lin et al. (2013) and others, who demonstrated that the estimates of a risk-based quantity like MAFE is unique for a structure and is independent of the IM choice or $Sa(T^*)$ conditioning period. This finding is subject to the conditions that: 1) the ground motion records used to quantify the structural response and estimate the MAFE are hazard-consistent, as was the case here; 2) the IM employed to be sufficient, which O'Reilly (2021) has shown for the IMs examined; and 3) for the IM to be an efficient indicator of the structural response, which was discussed in Figure 4(left). Therefore, for each of the IMs examined, the MAFEs would be expected to converge to the same value. Figure 4(right) shows these demand-hazard curves for the case study building using the three IMs considered. It shows how each IM reports a very similar value of risk at low demand levels, and gradually reduces with increasing demand before bottoming out at a value corresponding to the mean annual frequency of collapse. However, each curve gradual diverges from one another, with $Sa(T^*)$ reporting the highest estimate of risk for a given EDP and $Sa_{avg}(T^*)$ the lowest. This difference is attributed to the dispersion observed for each IM (Figure 4(left)), whereby the large dispersion observed for IMs such as $Sa(T^*)$ resulted in a higher estimate of the risk.

4.4. Bias

Given the observations regarding the IM dispersion in Figure 4(left) and the estimates of risk that the different IMs produce in Figure 4(right), it is of interest to know what the reasons for such a difference may be. Some dispersion is generally expected for all IMs due to the inherent randomness of ground motions, amongst other sources of uncertainty. However, there may be situations where dispersion may not necessarily be due solely to aleatory uncertainty but rather from other pertinent ground motion characteristics biasing the response. Bradley (2012) discussed bias within the context of ground motion record selection, noting how for some scenarios, the results obtained using ground motions selected and scaled to a single conditioning IM denoted IM_j (e.g. $Sa(T^*)$) could also be biased by another IM termed IM_i (e.g. ground motion duration).

This aspect was explored in depth by O'Reilly (2021) and is discussed here for the case-study building. In particular, the susceptibility of the structural to velocity-based ground motion characteristics is examined. Of the various velocity-based IMs available, filtered incremental velocity, *FIV3*, defined by Dávalos and Miranda (2019)was adopted. The shortcomings of IV surrounding its period independence, its local interruption of velocity pulses through high frequency-induced zero-crossings, and neglection of cumulative pulses were directly addressed.

For each of these MSA stripes with conditioning IM_j shown on the horizontal axis in Figure 3(left), the corresponding IM_i=*FIV3* values of each ground motion were plotted via markers on the vertical axis. This distribution of $IM_i|IM_j$ at each intensity is what indirectly results when selecting ground motions conditioned on IM_j alone. To examine bias due to IM_i=*FIV3*, the results were segregated based on the collapsing and non-collapsing cases. First, the median values of IM_i at each MSA stripe IM_j, $\eta_{IM_i|IM_j}$, were computed and plotted as the median trend for that IM_i. Then for the collapsed cases, their median value for each given MSA stripe at IM_j was computed as $\eta_{IM_i|IM_j,collapse}$. These are shown in Figure 5 for the case-study building with IM_i=*FIV3* in each case and IM_j = $Sa(T^*)$, *PGA* and $Sa_{avg}(T^*)$. This comparison illustrates the influence of the velocity-based characteristics of the ground motions on the collapse behaviour in a relatively simple manner. Should there be no biasing impact of IM_i=*FIV3* on the response analysis results, the medians will be closely aligned (i.e., $\eta_{IM_i|IM_j} \approx \eta_{IM_i|IM_j,collapse}$), where a biasing effect will show a deviation between the two (i.e., $\eta_{IM_i|IM_j} \neq \eta_{IM_i|IM_j,collapse}$).

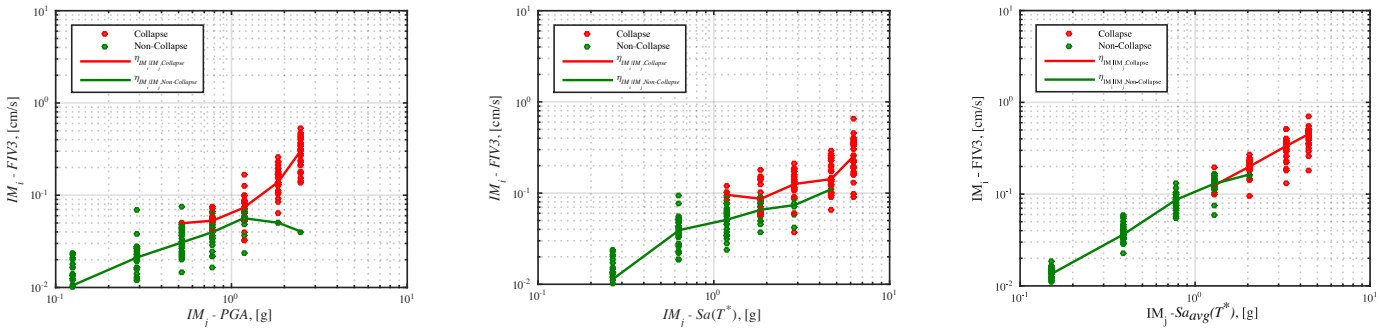

(a) *PGA* (b) *Sa*(*T**) (c) *Sa*$_{avg}$(*T**)

Figure 5. Comparison of the median IM$_i$ *values for a given* IM$_j$*, illustrating the potential bias in response due to* IM$_i$=FIV3

For the IMs examined, Figure 5 illustrates how for both *PGA* and *Sa*(*T**), there is a clear distinction in terms of *IM*$_i$=*FIV3* between the records causing collapse and those not. Also of note is the level of scatter in the *IM*$_i$=*FIV3* values for *PGA* and *Sa*(*T**) compared to *Sa*$_{avg}$(*T**). These results indicate that there is a biasing effect of the velocity-based IMs such as *IM*$_i$= *FIV3* on the *IM*$_i$=*Sa*(*T**) and *PGA* results, whereas *IM*$_i$= *Sa*$_{avg}$(*T**) did not present such an impact given that the collapse and non-collapse median trends align well. This is a notable observation as it indicates that the large dispersion observed in Figure 5 for each IM, and subsequent overestimation of risk in Figure 4(right), may be because for *PGA* and *Sa*(*T**), depending on the velocity-based characteristics of the selected ground motions, which are typically not considered in CS-based record selection, the collapsing cases can be notably impacted and biased. However, when using *Sa*$_{avg}$(*T**) as the IM, the results tended not to be biased in such a way, indicating that it may be a more suitable IM for assessing the response of infilled non-ductile RC frames. However, other record selection methods such as the generalised conditional intensity measure could be used, which can directly consider the velocity-based characteristics of records, given that they have been observed to have a notable impact on the results obtained.

5. Summary

This paper has examined the seismic assessment of an infilled reinforced concrete (RC) frame utilising different intensity measures (IMs). Examining the dispersion in intensities required to exceed a given drift demand, *PGA* was seen to have relatively high dispersion, *Sa*(*T**) showed efficiency initially but gradually became highly disperse, while *Sa*$_{avg}$(*T**) exhibited a relatively moderate dispersion throughout. Structural response when using *PGA* and *Sa*(*T**) as the IM were shown to depend on the velocity-based parameters of the ground motion records used. This supports previous findings regarding the large dispersion in the response of infilled RC frames. A similar analysis of the structural response when using *Sa*$_{avg}$(*T**) showed no such dependence, giving it a more consistent response prediction with reasonable dispersion and insensitivity to other ground motion parameters found to be problematic here. Overall, this study has shown that classic IMs like *PGA* and *Sa*(*T**) possess some issues when used as part of the risk-oriented assessment of infilled RC frames, whereas a new addition to seismic risk assessment, *Sa*$_{avg}$(*T**), was seen to indirectly dampen many of these issues without much extra effort.

Acknowledgements

This work has received support from the ROSSINI project, funded by INAIL (Italian national institute for workplace insurance) under the call "BRIC 2019".

References

Bradley, Brendon A. 2012. “The Seismic Demand Hazard and Importance of the Conditioning Intensity Measure.” *Earthquake Engineering & Structural Dynamics* 41 (11): 1417–37. https://doi.org/10.1002/eqe.2221.

Dávalos, Héctor, and Eduardo Miranda. 2019. “Filtered Incremental Velocity: A Novel Approach in Intensity Measures for Seismic Collapse Estimation.” *Earthquake Engineering & Structural Dynamics* 48 (12): 1384–1405. https://doi.org/10.1002/eqe.3205.

Jayaram, N., T. Lin, and J. W. Baker. 2011. “A Computationally Efficient Ground-Motion Selection Algorithm for Matching a Target Response Spectrum Mean and Variance.” *Earthquake Spectra* 27 (3): 797–815. https://doi.org/10.1193/1.3608002.

Kohrangi, Mohsen, Paolo Bazzurro, Dimitrios Vamvatsikos, and Andrea Spillatura. 2017. “Conditional Spectrum-Based Ground Motion Record Selection Using Average Spectral Acceleration.” *Earthquake Engineering & Structural Dynamics* 46 (10): 1667–85. https://doi.org/10.1002/eqe.2876.

Lin, Ting, Curt B. Haselton, and Jack W. Baker. 2013. “Conditional Spectrum-Based Ground Motion Selection. Part I: Hazard Consistency for Risk-Based Assessments.” *Earthquake Engineering & Structural Dynamics* 42 (12): 1847–65. https://doi.org/10.1002/eqe.2301.

Nafeh, Al Mouayed Bellah, Gerard J. O’Reilly, and Ricardo Monteiro. 2020. “Simplified Seismic Assessment of Infilled RC Frame Structures.” *Bulletin of Earthquake Engineering* 18 (4): 1579–1611. https://doi.org/10.1007/s10518-019-00758-2.

O’Reilly, Gerard J. 2021. “Limitations of Sa(T1) as an Intensity Measure When Assessing Non-Ductile Infilled RC Frame Structures.” *Bulletin of Earthquake Engineering* 19 (6): 2389–2417. https://doi.org/10.1007/s10518-021-01071-7.

O’Reilly, Gerard J., and Ricardo Monteiro. 2019. “Probabilistic Models for Structures with Bilinear Demand-Intensity Relationships.” *Earthquake Engineering & Structural Dynamics* 48 (2): 253–68. https://doi.org/10.1002/eqe.3135.

O’Reilly, Gerard J., Davit Shahnazaryan, Al Mouayed Bellah Nafeh, Volkan Ozsarac, Denis Sarigiannis, Paolo Dubini, Filippo Dacarro, et al. 2022. “Utilization of a Sensor Array for the Risk-Aware Navigation in Industrial Plants at Risk of Natech Accidents.” In *Proceedings of the ASME 2022 Pressure Vessels & Piping Conference PVP2022*. Las Vegas, Nevada, USA.

O’Reilly, Gerard J., and Timothy J. Sullivan. 2019. “Modeling Techniques for the Seismic Assessment of the Existing Italian RC Frame Structures.” *Journal of Earthquake Engineering* 23 (8): 1262–96. https://doi.org/10.1080/13632469.2017.1360224.

Regio Decreto. 1939. “Norme per l’esecuzione Delle Opere Conglomerato Cementizio Semplice Od Armato - 2229/39.” Rome, Italy.

Rossetto, T., and A. Elnashai. 2003. “Derivation of Vulnerability Functions for European-Type RC Structures Based on Observational Data.” *Engineering Structures* 25 (10): 1241–63. https://doi.org/10.1016/S0141-0296(03)00060-9.